Nonlinear dynamics of ruby NMR laser with external feedback

N. A. Loĭko and A. M. Samson

Stepanov Physics Institute, Belorussian Academy of Sciences

We investigate theoretically the possible operating regimes of a ruby NMR laser with a feedback injection signal that depends on the radiation field generated in a preceding instant of time determined by the time of passage of the signal through the feedback loop. We track the bifurcations experienced by the system when the delay time is changed. We determine the conditions for generating stable pulses and the pulse characteristics. We describe the course of the randomization and of the onset of multistabilities.

INTRODUCTION

The ruby NMR laser is recently attracting much attention as a test system for the study of regular and random regimes.[1-4] On the one hand, it demonstrates the variety of nonlinear effects under various single-mode lasing conditions. On the other, its dynamics can be adequately described by three or two Bloch–Kirchhoff equations with parameters close to the actual ones.[1,2] In particular, a number of peculiarities of the cycle-creation bifurcation was investigated in Ref. 2, using as an example an NMR laser controlled by an injected signal formed directly from the generated rf signal. To this end, the latter was fed into a supplementary fast-response feedback (FB) circuit containing an amplitude limiter, a precise attenuator, and a phase rotator. As a result, the injected field did not vary with time, the frequency coincided with that of the radiation field ($\omega \approx 80$ MHz), and the fixed phase difference between these fields was zero or π. In the former case the control field had the same direction as the laser field (cooperative field configuration). In the latter the fields were oppositely directed (competing configuration). A competing-configuration NMR laser turned out to be quite sensitive to variation of the parameters and a convenient tool for the study of many aspects of nonlinear dynamics in the vicinity of the point where the Andronov–Hopf subcritical bifurcation takes place (an unstable equilibrium state bifurcates to an unstable cycle that surrounds the stable equilibrium state).

We report here the results of a theoretical investigation of the dynamics of a modified system with FB; the system organizes a signal with an amplitude that depends on the emission field. We assume in addition that the FB circuit includes a delay line. It is known that the presence of retarded FB that controls one of the laser parameters enriches substantially the lasing dynamics (see, e.g., Refs. 5–9). We shall determine below the conditions under which such a control of the injected field can lead to various bifurcation phenomena, multistability, and chaos.

THE MODEL

We use as the basic model the single-mode ruby NMR laser described in Refs. 1 and 2. Its principal element is an Al_2O_3:Cr^{3+} crystal with an ensemble of spins of the ^{27}Al nucleus as the active medium. The crystal is placed inside the NMR coil of an LC circuit tuned to the frequency ω_a of the transition between the Zeeman levels produced by a static magnetic field with induction B_0. In the case of the transition $(1/2, -1/2)$ transition considered by us we have $\omega_a = gB_0$ (g is the gyromagnetic ratio of ^{27}Al). The resonant circuit acts as the laser cavity. The current induced in it by variation of the nuclear-magnetization vector produces an emission magnetic field $B(t)$ that acts on the ^{27}Al spin system. This interaction can be described by the Bloch equations in a (u,v,z) coordinate frame rotating relative to a field $\mathbf{B}_0 \| \mathbf{z}$ at an emission-field frequency ω:

$$\dot{M}_u = -\gamma_\perp M_u + \Delta\omega_a M_v - sgB_v M_z,$$

$$\dot{M}_v = -\gamma_\perp M_v - \Delta\omega_a M_u + sgB_u M_z, \tag{1}$$

$$\dot{M}_z = -\gamma_\| (M_z - M_e) + gB_v M_u - gB_u M_v.$$

Here M_u and M_v are subcomponents of the transverse component of the active-spin nuclear-magnetization vector, M_z its transverse component and proportional to the population difference to the Zeeman levels, M_e the magnetization produced by the pump, B_u and B_v components of the laser-field magnetic induction $\mathbf{B}(B_u, B_v, 0)$, $\gamma_\perp$ the rate of transverse relaxation, $\gamma_\|$ the rate of spin-lattice relaxation, $\Delta\omega = \omega_a - \omega$, and s is a spin factor equal to 9 for the given transition.

It is assumed that the magnetic induction of the laser field is equal to

$$B(t) = \frac{\mu N J_L(t)}{l}, \tag{2}$$

where $j_L(t)$ is the current in the NMR coil; l is the effective length of the winding, N the number of turns, and μ the induction constant. According to Kirchhoff's rules as applied to an LC circuit with feedback that transforms the output signal into a signal injected into the circuit through resistor R_0, the current J_L satisfies the equation

$$\ddot{J}_L + \frac{\omega_c}{Q}\left(1 + \frac{R_\|}{R_0}\right)\ddot{J}_L + \omega_c^2\left(1 + \frac{R_\|}{R_0 Q^2}\right)J_L$$

$$= \frac{\omega_c Q}{R_\|}\dot{V} + \frac{\omega_c^2}{R_0}(V + V_{FB}). \tag{3}$$

Here $\omega_c = 1/LC$ is the frequency of the circuit, $R_{\parallel}$ its effective parallel resistance, $Q = R_{\parallel}/\omega_c L$ the NMR coil which determines the damping constant $k = \omega_c/2Q$, and V the electromotive force induced in the coil by rotation of the magnetization vector, and equal according to Faraday's law to

$$V = -\mu\eta A N \frac{d}{dt}(M_u \cos \omega t + M_v \sin \omega t), \qquad (4)$$

where η is the space factor and A the transverse cross section of the NMR coil. The voltage V_{FB} injected via the feedback signal is determined by the loop voltage U_{LC}

$$V_{FB} = -\beta U_{LC}(t-\tau)\cos \omega\tau$$

$$= -\beta \cos \omega\tau \left[\frac{R_{\parallel}}{\omega Q} \dot{J}_L(t-\tau) + \frac{R_{\parallel}}{Q^2} J_L(t-\tau) \right.$$

$$\left. -V(t-\tau) \right], \qquad (5)$$

β is the FB coefficient, and τ is the time of passage of the signal through the FB circuit. We assume hereafter that $\omega\tau = 2\pi n$ or $\pi(2n+1)$, and include the corresponding sign in β.

Since the following conditions are usually satisfied in experiment:[1,2]

$$|\dot{M}_{u,v}| \ll |\omega M_{u,v}|, \quad R_{\parallel} \ll R_0, \qquad (6)$$

Eq. (3) reduces, with sufficiently good approximation, to a first-order equation for a slowly varying amplitude of the current I ($J_L = I \exp(-i\omega t) + I^* \exp(i\omega t)$). Taking (2) into account, we obtain the connection between I and the generated-field magnetic-induction components B_u and B_v:

$$B_u = \frac{\mu N}{2l}(I+I^*), \quad B_v = \frac{\mu N}{2l}(I-I^*), \qquad (7)$$

and write the equation for the field characteristics. It takes in the case of exact resonance the form

$$\dot{b} = -k_1 \left[b - i\widetilde{m} - \alpha b(t-\tau) - \frac{i\alpha}{Q}b(t-\tau) + \frac{\alpha}{Q}\widetilde{m}(t-\tau) \right]. \qquad (8)$$

We have introduced here new dimensionless variables

$$b = (B_u + iB_v)3g/\gamma_{\parallel} = 3g\mu NI/l\gamma_{\parallel},$$

$$m = (M_u + iM_v)3g\mu\eta Q/2\gamma_{\parallel};$$

the time is normalized to $1/\gamma_{\parallel}$, $k_1 = k/\gamma_{\parallel}$ is a parameter, and $\alpha = R_{\parallel}\beta/R_0$ is indicative of the depth of feedback. Usually $|\alpha| \ll 1$. The system (1) reduces here to

$$\dot{\widetilde{m}} = -\gamma\widetilde{m} + ibz,$$

$$\dot{z} = -z + \lambda + \frac{i}{2}(\widetilde{m}b^* - \widetilde{m}^*b), \qquad (9)$$

where

$$z = \frac{9g\mu\eta Q}{2\gamma_{\parallel}}M_z, \quad \gamma = \gamma_{\perp}/\gamma_{\parallel}, \quad \lambda = \frac{9g\mu\eta Q}{2\gamma_{\parallel}}M_e.$$

According to Refs. 1 and 2 the field-damping is $k_1 \gg \gamma \gg 1$. This permits an adiabatic exclusion in (8), so that

$$b = i\widetilde{m} - \alpha \left[b(t-\tau) + \frac{i}{Q}\dot{b}(t-\tau) + \frac{1}{Q}\widetilde{m}(t-\tau) \right]. \qquad (10)$$

A solution of (10) can be obtained by expanding b in terms of the small parameter α. The result is

$$b = i\widetilde{m} - i\alpha\widetilde{m}(t-\tau). \qquad (11)$$

Substituting (11) in (9), choosing the initial conditions such that $B_v(t=0)=0$ ($M_u(t=0)=0$), and introducing the real variable $m = -i\widetilde{m}$, we obtain the final system for the description of the dynamics of the investigated laser:

$$\dot{m} = -\gamma m - zm + \alpha zm(t-\tau),$$

$$\dot{z} = -z + \lambda + m^2 - \alpha zm(t-\tau). \qquad (12)$$

Equations (12) are similar to those obtained in Ref. 2 for an NMR laser with constant injected signal, if the magnetic-induction $b = -m + am(t-\tau)$ is regarded as the sum of the inductions of the field $b_g = -m$ generated at the given instant of time and the field $b_i = am(t-\tau) = -\alpha b_g(t-\tau)$ of the injected signal. If $\alpha < 0$ the feedback preserves the injected-signal phase, which is equal to the emission-field phase at the instant $t-\tau$. When $\alpha > 0$ the corresponding phase is shifted by π.

The NMR-laser output voltage picked off the LC circuit is first applied to an rf rectifier. The resultant output signal is proportional under the above assumptions to the transverse components of the nuclear susceptibility m.

EQUILIBRIUM STATES

For $-\lambda < \gamma/(1-\alpha)$ the set (12) of equations with delay has one trivial equilibrium state: $m_T = 0$, $z_T = \lambda$. When the pump parameter $|\lambda|$ reaches a value $\gamma/(1-\alpha)$ a fork-type bifurcation leads to two more states:

$$m_0^{\pm} = \pm(u_0)^{1/2} = \pm[(z_0-\lambda)/(1-\alpha)]^{1/2},$$

$$z_0 = -\gamma/(1-\alpha). \qquad (13)$$

They correspond to generation of counterpropagating fields with magnetic-induction vector constant in time. The trivial solution becomes unstable in this case. If $\alpha < 0$ for both solutions (13), the phase difference between the injected and generated fields is zero, i.e., a cooperative configuration of these fields is effected. Just as the case of an injected signal constant in time,[2] in this configuration the equilibrium states are stable in almost the entire accessible range of parameter variation [instability sets in only at relatively large feedback depth α, when the conditions for transforming to the set of equations (12) no longer hold]. All the bifurcation phenomena of interest take place when the solutions (13) accord with the competing field configuration ($\alpha > 0$).

The stability of the equilibrium states (13) is determined by the roots of the characteristic quasipolynomial

$$[p - a(1 - \exp^{-p\tau})](1+p) + d + c\exp^{-p\tau} = 0, \qquad (14)$$

where $a = -\alpha z_0$, $d = u_0(1-\alpha)(2-\alpha)$, $c = -u_0(1-\alpha)\alpha$.
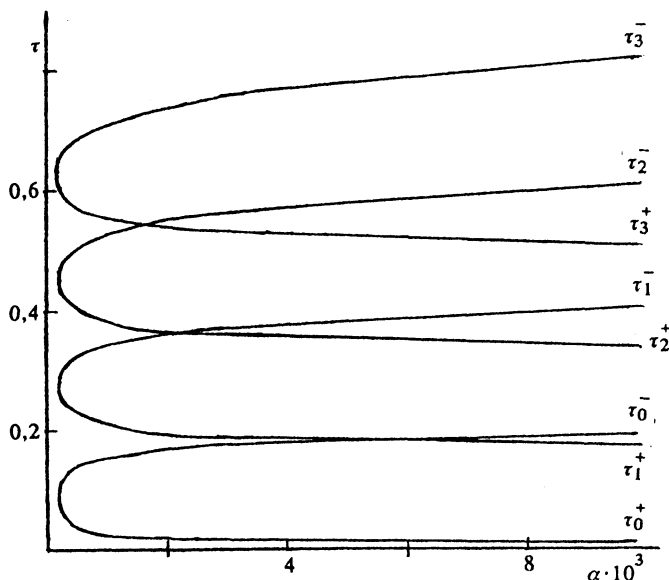
FIG. 1. Bifurcation curves (15)–(16) for $\gamma = 2.4 \cdot 10^3$ and $\lambda = -3 \cdot 10^3$.

Using the method of D-partition[10] in the parameter space of the system one can separate regions with different orders of stability (different number of roots $p_n = x_n \pm iy_n$ with $x_n > 0$, $n = 0$, 1, 2...). The corresponding boundary curves where x_n reverses sign take for each n the form

$$\tau_n^{\pm} = \frac{1}{y_{\pm}} \operatorname{arctg} \frac{y_{\pm}[c(1-a)+a(1-d)]+ay_{\pm}^3}{y_{\pm}^2(a^2+c)-(d-a)(a+c)} + \frac{2\pi n}{y_{\pm}}. \tag{15}$$

The arctangent is chosen here in the interval $[0,2\pi]$ in accordance with the sign of $\sin y_{\pm}\tau \sim ay_{\pm}^2 + c(1-\alpha) + \alpha(1-d)$, $y_{\pm} > 0$ and is equal to y_n on the bifurcation boundary $x_n = 0$:

$$y_{\pm}^2 = \tfrac{1}{2}(2d-1)$$

$$\pm \{\tfrac{1}{4}(2d-1)^2 - [(d^2-c^2) - 2a(d+c)]\}^{1/2}. \tag{16}$$

Figure 1 shows plots of (15) and (16) with $n = 0$, 1, 2, 3 for typical parameters of a ruby NMR laser.[1,2] The $x_n > 0$ regions are bounded by two branches τ_n^+ and τ_n^-. The equilibrium states are stable at low feedback depths ($\alpha \lesssim 3 \cdot 10^{-4}$). As α increases bounded intervals of τ appear, in which one of the roots has a positive real part and the corresponding partial solution of the linearized system oscillates with frequency y_n close to the frequency $\omega_r = [-2(\lambda + \gamma)]^{1/2}$ of the relaxation oscillations of the laser without feedback. With further increase of α these intervals overlap partially. A larger number of roots with positive real part raises the order of the system instability.

Note that instability occurs mainly at delay values $\tau \gtrsim \gamma^{-1}$ Following Ref. 11, with allowance for the fact that the longitudinal component of the magnetization changes little relative to the threshold value $-\gamma/(1-\alpha)$, the first equation can be reduced adiabatically to the difference equation

$$m(t) = \alpha z/(\gamma + z)m(t-\tau). \tag{17}$$

The equation for z takes then the form

$$\dot{z} = -z + \lambda - \gamma m^2/z. \tag{18}$$

In view of the foregoing, the value of $|\alpha z/(\gamma + z)|$ remains close to unity all the time. If $\alpha z/(\gamma + z) \approx 1$, Eq. (17) describes a mapping of the function $m(t)$. Its fixed points $[m_0(t) = m_0(t-\tau)]$ coincide with the equilibrium states (13) of the initial system and describe stable time-constant solutions. The mapping for $m(t)$ takes at $\alpha z/(\gamma + z) \approx -1$ the form

$$m(t) = \frac{\alpha z}{(\gamma + z)}^2 m(t-2\tau). \tag{19}$$

The corresponding fixed points

$$m_1^{\pm} = \pm (u_1)^{1/2} = \pm [(z_1 - \lambda)/(1+\alpha)]^{1/2},$$
$$z_1 = -\gamma/(1+\alpha) \tag{20}$$

describe stable 2τ-periodic solutions shifted apart by half a period. They are characterized by a constant value of $|m|$ and a jumpwise reversal of the sign of m at time intervals equal to τ:

$$m(t) = -m(t-\tau) = m_1^{\pm}. \tag{21}$$

The generated signal has the form of rectangular pulsations. By virtue of relation (21), a cooperative field configuration is realized. It is natural to expect the solution of the system of differential-difference equations (12) to tend (asymptotically as τ, $\gamma \to \infty$) to the solution (20), (21). The feasibility of its realization, as well as that of other solutions of the system (12), was investigated by numerical integration. The results are summarized below.

BASIC BIFURCATIONS

We consider first small FB depths, when u_0 and z_0 are respectively close to u_1 and z_1. The intervals of τ in which the equilibrium states (13) are unstable do not overlap as a rule in this case (Fig. 1). Let us track the bifurcations that occur in the system (12) when the delay time is varied (Fig. 2a). As indicated above, at small τ the solutions (13) are stable. They lose stability at the point $\tau = \tau_0^+$, where each of the solutions undergoes a subcritical Andronov–Hopf bifurcation. Unstable cycles are produced when τ decreases from the value τ_0^+. They separate attraction wells for three stable solutions coexisting in a narrow delay interval $[\tau_{0.1}, \tau_0^+]$, two equilibrium states (13) and a periodic regime. The latter is characterized by abrupt bursts of magnetization m (or field b) symmetric about a zero value and separated by a time interval much longer than τ and $T_r = 2\pi/\omega_r$ (Fig. 3a).

The value of m fluctuates about zero in the intervals between the pulses. Since τ is small compared with the pulsation period $m(t)$, the injected field, which is proportional to $m(t-\tau)$, is mainly in counterphase to the generated the generated field, except in the instants when the sign of $m(t)$ is reversed. The corresponding phase trajectory encloses both stationary states. If, following Ref. 12,
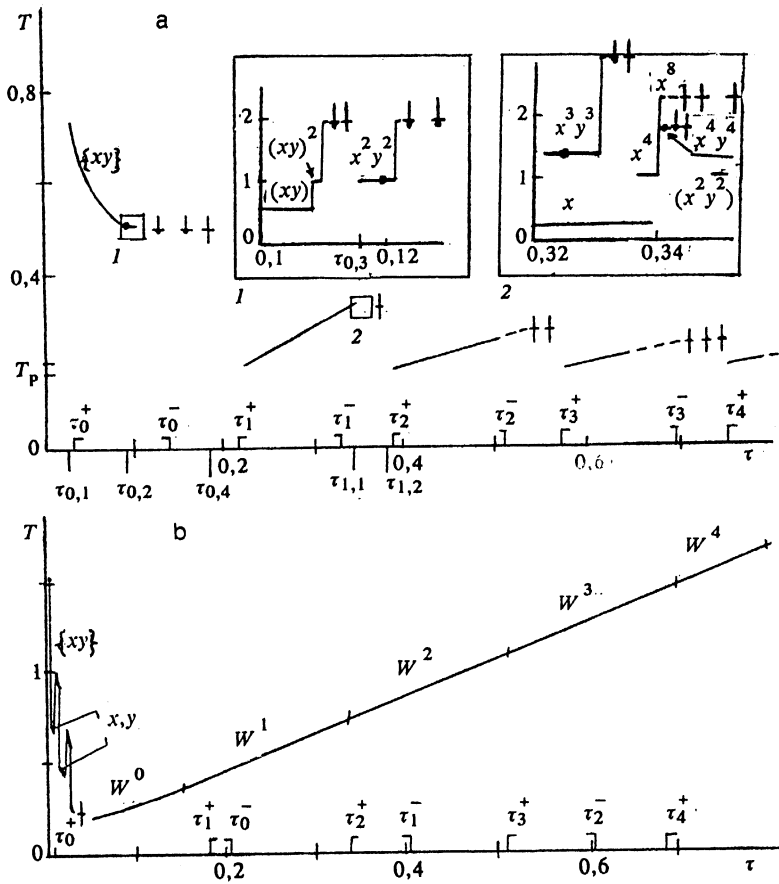
N. A. Loĭko and A. M. Samson   30

FIG. 2. One-parameter diagram of bifurcations for $\alpha = 5 \cdot 10^{-4}$ (a) and 10^{-2} (b). The remaining parameters are those of Fig. 1.——periods T of stable pulsations;— — quasiperiodic motion; ⊥ —asymmetric chaotic motion; †—symmetric chaotic motion ●—symmetry loss bifurcation.

we denote by x each turn of the trajectory during the period around the state m_0^+, by y each turn around the state m_0^-, and by the braces symmetric orbits, the symbol of the given attractor will be $\{xy\}$. We refer to this branch of periodic solutions as the zeroth, since the region of its existence practically coincides with the instability region of the equilibrium states (13) with $n=0$. The amplitude and the period of the oscillations decrease in motion along this branch toward decreasing τ (see Fig. 2a). At $\tau = \tau_{0.2}$ the cycle $\{xy\}$ becomes unstable as a result of bifurcation of the symmetry loss.

Two asymmetric cycles (xy) and (yx) are produced (the parentheses denote here asymmetry of the oscillations about the zero value of the magnetization m), one of which is shown in Fig. 3b. The presence of a pair of cycles, as well as of solutions (13) that go over into one another upon reversal of the sign of m, is due to the invariance of Eqs. (12) to the substitution $m \to -m$ or to a change of the field phase by π. These cycles undergo next successive period doubling bifurcations $(xy)^{2n}$ and $(yx)^{2n}$, leading to two asymmetric random attractors. As τ increases further, increases take place in both the scatter of the extremal values of the pulsating magnetization and in the number of jumps of the phase trajectory from the vicinity of one equilibrium to that of another with a different sign of m, until the attractors coalesce into one symmetric random attractor. At $\tau = \tau_{0.3}$ it bifurcates to a periodic symmetric orbit $\{x^2 y^2\}$ (Fig. 3c). Finally, the succeeding bifurcations of symmetry loss and of period doubling of the type $(x^2 y^2)^{2n}$ again lead

to two asymmetric random sets, which converge subsequently into one (Fig. 3d).

The Andronov–Hopf bifurcation on the upper boundary of the interval of instability with $n=0$ at the point τ_0^- is also subcritical. Unstable cycles are produced in this case when τ increases. A chaos coexisting with two equilibrium states is preserved in the interval $[\tau_0^-, \tau_{0.4}]$.

In contrast to the zeroth mode of the periodic solutions of the system (12), the first mode is produced "softly" via a supercritical Andronov–Hopf bifurcation at the point $\tau = \tau_1^+$ (Fig. 2a). Both equilibrium states (13) lose stability and two stable cycles x and y, are generated, with opposite signs of the magnetization m, each enclosing a corresponding immobile point.

An example of such a solution is shown in Fig. 3e. The magnetization m oscillates without change of sign (vector direction). A competing configuration of an injected field and a generated one is produced. The pulsation period $\approx \tau$ is close to $T_r = 2\pi(\omega_r)$, i.e., the relaxation oscillations of the laser are amplified by resonance with the feedback natural frequency $2\pi/\tau$. The pulsation amplitude increases with the delay τ. The solutions remain stable up to the value $\tau = \tau_{1,1}$, which exceeds the upper limit τ_1^- of the instability interval of the states (13) with $n=1$ in which a subcritical Andronov–Hopf bifurcation takes place anew. Multistability is observed in the vicinity of this point, viz., coexistence of the τ-cycles and a pair of solutions a fourfold period x^4 and y^4. The numerical experiment revealed
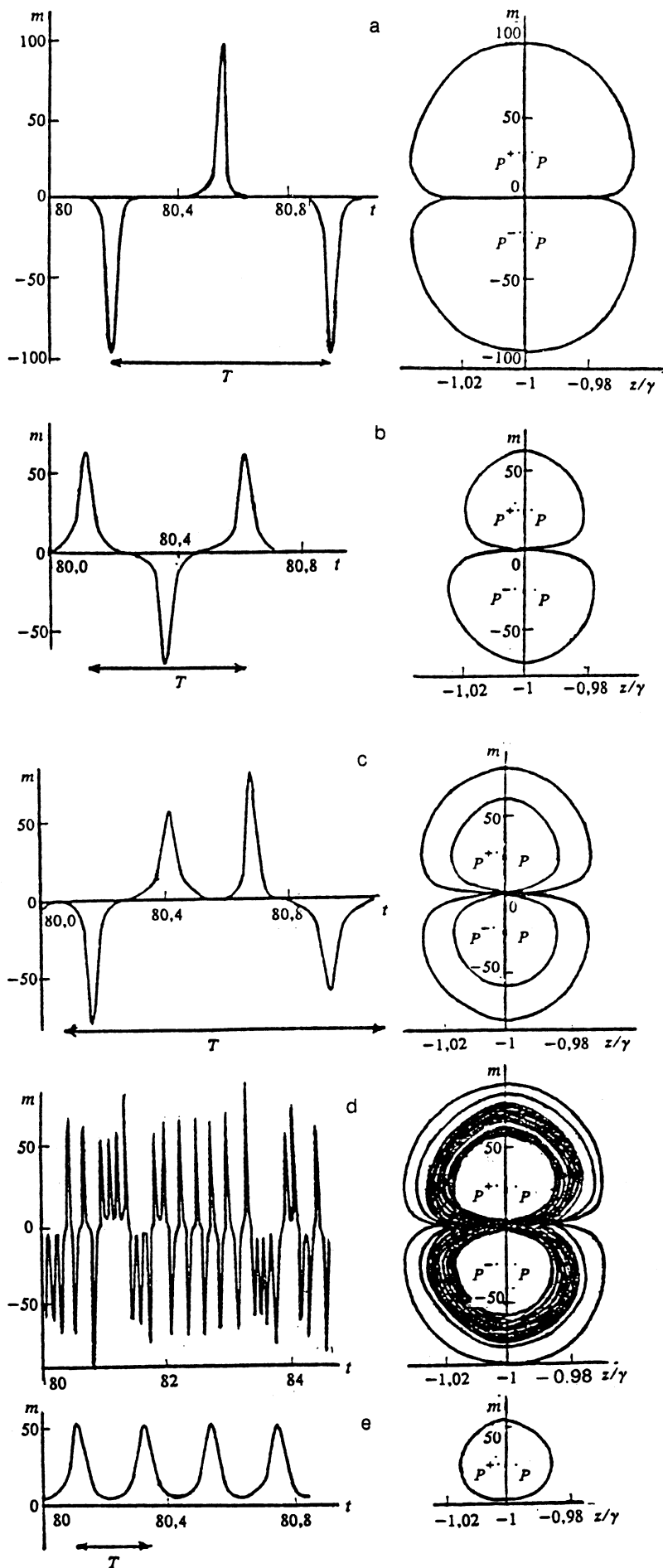
FIG. 3. Shapes of pulsations $m(t)$ and corresponding phase portraits at $\alpha=5\cdot10^{-4}$ and $\tau=0.04$(a), 0.1(b), 0.116(c), 0.17(d), 0.25(e). The remaining parameters are those of Fig. 1. $P^{\pm}$—immobile points (13), P—projection of solution (20), (21).
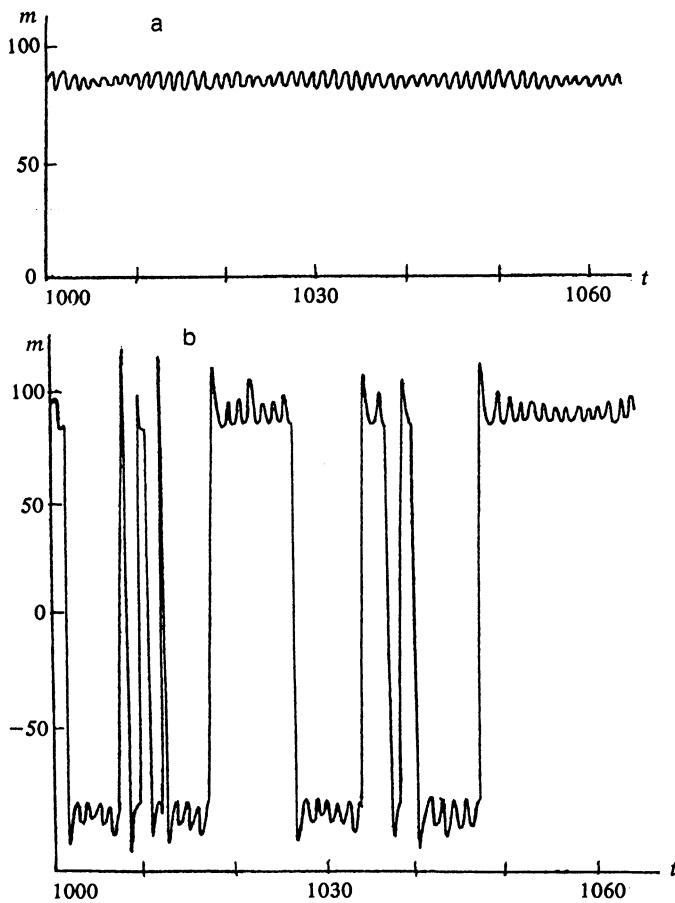
FIG. 4. Envelope of maximum pulsations $m(t)$ for $\alpha=5\cdot10^{-4}$ and $\tau=0.3423$(a), 0.343(b).

next a 4τ period-doubling bifurcation and a soft transition to two quasiperiodic solutions close to the cycles x^8 and y^8 of period 8τ (Fig. 3a).

When the parameter τ exceeds a certain critical value, these solutions interact and the result is reversal of the direction of the magnetization vector and a change of the phase of the generated signal by π. The system stays initially a rather long time on one of the quasiperiodic orbits, goes over next to another orbit with opposite sign of m, and so forth. These transitions are irregular in time and are characterized by an increase of the pulsation amplitude (Fig. 4b). This corresponds to the presence of relatively long laminary phases of quasiperiodic motion, interrupted by irregular flashes, i.e., a "quasiperiodicity-chaos" alternation.[13] The frequency of the reversal of the sign of m in individual time intervals and the durations of these intervals increase with increase retardation τ and the system goes over into a symmetric chaotic motion similar to that shown in Fig. 3d. The chaos exists up to the point $\tau_{1,2}$ of its annihilation with an unstable orbit separating the wells of attraction of the random set and the equilibrium states (13). A regularity window with an (x^2y^2) regime was observed at $\tau\approx0.35$. In addition, supplementary insulated branches of periodic solutions, $\{x^3y^3\}$ and $\{x^4y^4\}$ exist in the vicinity of the bifurcation boundary τ_0^- (Fig. 2a, inset

2). When the delay τ is increased, they undergo bifurcation sequences analogous those described above for the solutions $\{xy\}$ and $\{x^2y^2\}$ on the zeroth branch: loss of symmetry, doubling bifurcation of the period of each of the asymmetric cycles, coalescence of two asymmetric chaotic attractors.

The succeeding branches of the periodic solution are also generated softly at the points τ_n^+ on account of the supercritical Andronov–Hopf bifurcations (Fig. 2a, $n > 1$). The physical mechanism of their onset is resonant amplification of relaxation oscillations at a frequency ω_r close to one of the natural feedback frequencies $2\pi n/\tau$. On each branch there exist two τ/n cycles with opposite signs of m. The character of the oscillations is similar to that shown in Fig. 3e. As the delay τ is increased, these solutions, just as for $n=1$, bifurcate to two quasiperiodic orbits which interact subsequently through intermittency, creating a symmetric chaotic attractor. The chaos region contains windows of regular motion with symmetric and asymmetric trajectories of type x^ky^k. The upper limits of the instability intervals τ_n^- of immobile points are characterized by subcritical Andronov–Hopf bifurcations, so that the complex motion on the nth branch coexists with stable equilibrium states (13) practically up to values of τ_{n+1}^+. With increase of the number n of the solution, and hence of the delay time τ, the interval of τ in which a solution with period τ/n exists becomes shorter, and quasiperiodic and irregular oscillation regimes become more typical.

Note that in the considered case of small feedback depths α no solutions close to the solution (20), (21) of the simplified system (17), (18) were observed even for relatively long $\tau\gg\gamma^{-1}$ (at least within the limits of the investigated delay up to $\tau\approx2$). The dynamics of the system (12) is determined mainly by the character of the bifurcations of the immobile points (13). In view of the proximity of u_1, z_1 (20) to u_0, z_0 (13) the phase trajectories of the existing lasing regimes enclose both types of equilibrium states (Fig. 3).

An increase of α leads first of all to divergence of the values of the longitudinal magnetizations z_0 and z_1, and as a consequence to an increase of the distance between the corresponding points in the phase space of the system. For certain parameters this makes it possible to realize phase trajectories only in the vicinity of the projection of the solution (20), (21). Thus, in the region of the existence of the zeroth branch of the solutions, where the delays τ are small enough and are comparable with γ^{-1}, neither a transition from the system of equations (12) to the simplified system (17), (18) nor the presence of a solution (20), (21) is right. The dynamics is determined as before by the states (13). The basic structures of the solution duplicate those shown in Figs. 3a–3d. The range of variation of z is large and the phase trajectories, just as for small α, enclose the points m_0, z_0 and m_1, z_1. Only pairs of solutions x and y are noted and represent in fact $\{xy\}$ solutions (Fig. 3a) with values of m reversed every other pulse to the positive or negative m, respectively, and with half the period. The intervals where such solutions exist alternate with intervals where $\{xy\}$ solutions exist (Fig. 2b). The larger α, the

N. A. Loĭko and A. M. Samson   33

more frequent the alternation of these regimes with increase of τ, until symmetry-loss bifurcation sets in, i.e., a transition to a pair of coexisting solutions (xy) and (yx). The scenario of the transition to chaos duplicates subsequently the one described above for small α. With increase of α, at the end of the zeroth branch after the reverse cascade of period-doubling bifurcations, of the period, or via a "cycle-chaos" alternation,[13] a new type of regular symmetric solution takes place, with a period that tends to 2τ when the delay is increased. The phase trajectory shifts gradually relative to the immobile points (13). Starting with a certain α, it encloses only the projection of the solution (20), (21) (Fig. 5a).

We track now the corresponding changes in the regions of instability with $n > 1$. As indicated above, as the FB depth increases these regions overlap partially, leading to a larger interaction of the τ/n-periodic solutions. The stability intervals of these solutions decreases. When α exceeds a certain value $\approx (3-4) \cdot 10^{-3}$, a quasiperiodic or chaotic regime with small regularity windows is observed for practically all $\tau > \tau_1^+$. In these windows are realized regimes both with structure of type $(x^k y^k)$, determined mainly by the equilibrium states (13), as well as 2τ-periodic oscillations. In the latter case a fine structure appears in the segments of the time τ where $m(t)$ does not reverse sign, namely, pulsations attenuating towards values m_1^+ or m_1^- (Fig. 5b). After several contracting loops around the point (m_1^+, z_1) the phase trajectory goes over into the region of the point (m_1^-, z_1) etc. The solution tends to become discontinuous, with sections of slow and fast changes of the variable, characteristic of singularly perturbed systems with small parameters preceding the derivative. We denote such solutions by W^k, where k is the number of turns in the time τ. Further increase of α leads to formation of one branch of 2τ-periodic solutions, along which the number of rotations of the phase trajectory around the points $(m_1^\pm, z_1)$ increases (Fig. 2b). A certain correlation is observed then between the number k of turns and the number of the solution of the linearized system, i.e., the period of the fine structure is $\approx \tau/n$ and is close to the period T_r of the relaxation oscillations. The form of the $m(t)$ signal becomes more and more rectangular, with a strong spike on the leading front of the pulse (Fig. 5c). The solution of the system of differential-difference equations (12) becomes close to the solution (20), (21).

Thus, for relatively large α the main solution corresponds to a cooperative configuration of the fields in a laser with an external signal, a solution that turns out to be more stable, just as in the case of a signal constant in time.[2] Even at very large $\alpha \approx 0.1$, only an insignificant "breathing" is observed in the values of the spikes $m(t)$.

The proximity of the system (12) at large α and τ to the difference system (17), (18) predetermines the presence of harmonics with a period $2\tau/(2l+1)$ ($l = 0,1,2,...$) and of isomers [solutions with a period $\approx 2\tau/(2l+1)$ ($l = 0,1,2,...$)] and isomers (solutions with period $\approx 2\tau$, but of more complicated structure).[11] Without dwelling on a proof of this fact, which is given in Ref. 11 for an equation of the type of (17), we note that such solutions were in-

deed obtained by numerical integration of (12) (see, e.g., Fig. 5d). This, however, calls for imposition of special initial conditions. Thus, with change of the feedback depth α the system changed over to isomeric branches from a W-branch, and to harmonic branches from isomeric ones. When a constant magnetization m of any size was specified, only a W solution was realized on the segments $[-\tau, 0]$.

CONCLUSION

We have proposed a theoretical model of a ruby NMR laser with injectable signal controlled by retarded feedback. The lasing dynamics was studied in detail on the basis of formulated differential-difference equations. We have shown that at relatively large feedback depths there is realized mainly a cooperative field configuration (the phase difference between the generated field and the injection field is zero). Just as in the case of a time-constant signal,[2] this configuration is characterized by stable solutions. In contrast to Ref. 2, however, where such a solution was one of the nonzero equilibrium states (constant nuclear magnetization and constant NMR-laser output signal), the principal regime here is 2τ-periodic with asymptotically (as the delay τ increases) constant longitudinal component of the magnetization and output-signal amplitude. The phase of the latter, just as of the magnetization, changes by π every segment of the time τ. The presence of harmonics with a period $2\tau/(2l+1)$ and of isomers brings about multistability.

The competing configuration of the injectable and generatable fields (the difference of their phases is π) predominates at a low depth of feedback. Corresponding to such a configuration are the constant-time solutions (13) as well as regimes with periods τ/n. Just as in the case of a constant injectable signal, we have here regions of stability and instability of the given solutions. Equilibrium states can lose stability via supercritical or subcritical (as in Ref. 2) Andronov–Hopf bifurcation. As a result, stable equilibrium states can coexist with periodic limit cycles or with a random set. Chaos is produced as a rule via creation of two quasiperiodic orbits with opposite signs of magnetic induction of the pulsating laser field and interaction of these orbits. For relatively small delays τ, the system can generate more complicated periodic structures which are difficult to relate to the aforementioned two field configurations. Their creation and annihilation can also be accompanied by multistability and, as a consequence, by hysteresis.

The results indicate that the considered laser system enriches substantially the ruby NMR laser generation spectrum. This extends is field of application and utility for the study of bifurcation phenomena and multistability.

Note that the presented mathematical model of a self-oscillating system with delay can describe also other realistic devices or processes. For example, it is similar to the model proposed in Ref. 14 for the analysis of dynamic regimes in a laser whose active layer is significantly thinner than the emission wavelength. Our present results can therefore be of value when it comes to determine trends in
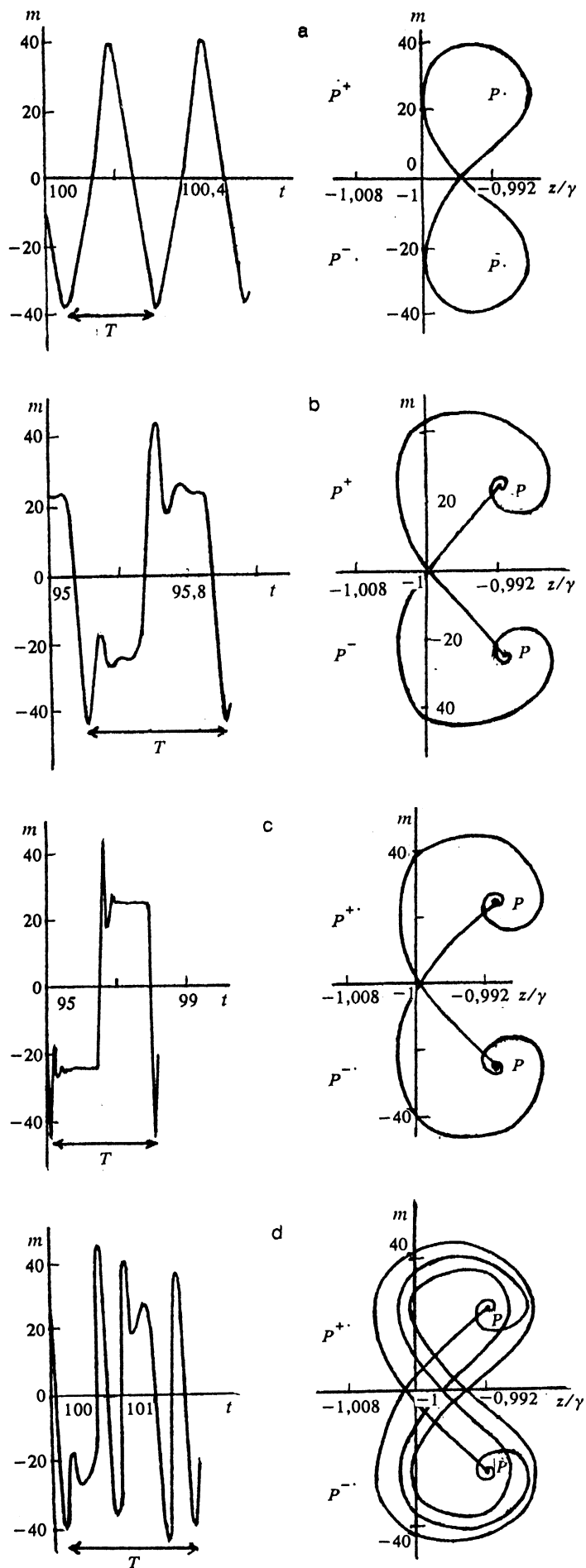
FIG. 5. Form of pulsations $m(t)$ and corresponding phase portraits for $\alpha = 10^{-2}$ and $\tau = 0.1$(a), 0.37(b), 1.5(c). The remaining parameters are those of Fig. 1. $P^{\pm}$—immobile points (13), P—projection of solution (20)–(21).

N. A. Loĭko and A. M. Samson   35

the development of the dynamics not only in NMR lasers, but in similar systems of different nature. On the other hand, the investigations[14] of equilibrium states in the case of arbitrary detuning of a laser-transition frequency points to the possibility of obtaining regimes that differ from those described above, which call for further study.

[1] E. Brun, B. Berighetti, D. Meier *et al.*, J. Opt. Soc. Am. B **2**, 156 (1985).

[2] R. Holzner, B. Berighetti, M. Ravani, and E. Brun, Phys. Rev. A **36**, 1280 (1987).

[3] A. Baugher, F. Hammack, and J. Lin, *ibid.* A **39**, 1549 (1989).

[4] Peter A. Braza and Erneux Thomas, *ibid.* A **40**, 2539 (1989).

[5] E. V. Grigor'eva, N. A. Loiko, and A. M. Samson. Preprint No. 548, Phys. Inst. Belorus. Acad. Sci., Minsk (1989).

[6] E. V. Grigor'eva, S. A. Kashchenko, N. A. Loiko, and A. M. Samson, Kvantovaya Elektron. (Moscow) **17**, 1023 (1990) [Sov. J. Quantum Electron. **20**, 938 (1990)].

[7] G. Giacomelli, M. Calzavara, and F. T. Arrecchi, Optics Comm. **74**, 97 (1989).

[8] F. T. Arecchi, G. Giacomelli, A. Lapucci, and R. Meucci, Phys. Rev. A **43**, 4997 (1991).

[9] N. A. Loiko and A. M. Samson, Preprint No. 635, Phys. Inst. Belorus. Acad. Sci., Minsk (1991).

[10] Yu. I. Neimark, *Dynamic Systems and Controllable Processes* [in Russian], Nauka, Moscow (1978).

[11] K. Ikeda and K. Matsumoto, Physica D **29**, 223 (1987).

[12] C. Sparrow, *The Lorenz Equation: Bifurcations, Chaos, and Strange Attractor*, Applied Mathematical Sciences, Vol. 41, Springer, New York (1982).

[13] P. Berger, I. Pomo, and C. Vidal, *Order in Chaos* (Russ. transl.), Mir, Moscow (1991).

[14] A. N. Oraevskii, Laser Physics **2**, 205 (1992).

Translated by J. G. Adashko